664202

DP-1090

27

AEC RESEARCH AND DEVELOPMENT REPORT

THERMAL NEUTRON DIFFUSION IN LIGHT AND HEAVY WATER

P. B. PARKS
D. J. PELLARIN
N. H. PROCHNOW
N. P. BAUMANN

DUPONT
REG. U. S. PAT. OFF.

Savannah River Laboratory

Aiken, South Carolina

LEGAL NOTICE

Printed in the United States of America
Available from
Clearinghouse for Federal Scientific and Technical Information
National Bureau of Standards, U. S. Department of Commerce
Springfield, Virginia 22151
Price: Printed Copy $3.00; Microfiche $0.65

664202

DP-1090

Physics
(TID-4500)

THERMAL NEUTRON DIFFUSION IN LIGHT AND HEAVY WATER

by

P. B. Parks
D. J. Pellarin
N. H. Prochnow*
N. P. Baumann

Approved by

B. C. Rusche, Research Manager
Experimental Physics Division

February 1968

*Present address: Wisconsin State University,
River Falls, Wisconsin

E. I. DU PONT DE NEMOURS & COMPANY
SAVANNAH RIVER LABORATORY
AIKEN, S. C. 29801

CONTRACT AT(07-2)-1 WITH THE
UNITED STATES ATOMIC ENERGY COMMISSION

ABSTRACT

The thermal neutron diffusion coefficients for H_2O and D_2O were determined from static measurements of the neutron relaxation length in boron-poisoned H_2O and D_2O and pulsed measurements of the neutron die-away in different-sized containers of these two moderators. The H_2O results agree well with previous measurements and fairly well with theory. The diffusion coefficients determined for H_2O are:

$$D_o = 3.57 \pm 0.04 \times 10^4 \text{ cm}^2 \text{ sec}^{-1}$$

$$C = 3.31 \pm 0.15 \times 10^3 \text{ cm}^4 \text{ sec}^{-1}$$

$$F = 2.8 \pm 0.7 \times 10^2 \text{ cm}^6 \text{ sec}^{-1}$$

The D_2O results agree reasonably well with calculations in the range of poison concentrations $\Sigma_a(B) = -0.04$ to $+0.04$ cm^{-1}. The restricted diffusion coefficients determined for D_2O are:

$$D_o = 2.09 \pm 0.02 \times 10^5 \text{ cm}^2 \text{ sec}^{-1}$$

$$C = 6.6 \pm 0.03 \times 10^5 \text{ cm}^4 \text{ sec}^{-1}$$

The pulsed measurements for D_2O resolved a previous discrepancy between pulsed and static determinations of D_o. The static measurements included neutron spectral index determinations as a function of neutron source and poisoning conditions. The theoretically predicted strong dependence of spectral indices on neutron source conditions in D_2O was verified. Evidence was also found for the existence of a pseudo energy equilibrium distribution in heavily poisoned D_2O. Normal analysis of this unusual data led to an assignment of the inverse diffusion length, κ, which exceeded Corngold's limit at $\kappa = \Sigma_s$, the free atom scattering cross section.

CONTENTS

LIST OF TABLES AND FIGURES

INTRODUCTION

Neutron relaxation lengths in poisoned moderating media and pulsed neutron decay constants in unpoisoned media are often measured to determine thermal neutron diffusion coefficients. However, these measurements can be misinterpreted because of improper treatment of angular distribution effects and variations in the neutron energy spectrum. The angular effects can be easily corrected by straightforward transport theory calculations, but the equilibrium spectra depend on the complex mechanisms of both the energy transfer to and from the moderating atoms (Scattering Kernel) and the nature of the static source feed.

In earlier Savannah River Laboratory (SRL) measurements[1] of the relaxation length of thermal neutrons in lightly poisoned D_2O, corrections were made for the poison-induced shifts in the energy spectrum as well as for the transport effects. However, the spectral correction used Westcott's relation derived for the high-energy source feed normally found in multiplying systems. Honeck and Michael[2] have pointed out that, for the thermal source actually used, the use of Westcott's relation leads to too large a correction. The resulting error in the reported SRL measurements was, nevertheless, within the quoted errors. Experiments have been designed to verify the extent to which source conditions affect the interpretation of the measurements.

Honeck[3] has treated the relationship of the effective diffusion coefficient and poison concentration by integral transport calculations in which he assumed a thermal feed; but, for the SRL measurements, the added poison was so small that Honeck's derived D_2O coefficients could not be verified on the basis of the SRL data alone. Existing pulsed measurements[4,5,6] on D_2O did appear to support Honeck's calculation of the energy shift (as represented by the cooling coefficient, C) but were questionable because the pulsed diffusion coefficient for zero spectral shift, D_o, disagreed with that derived from static measurements. The average pulsed diffusion coefficient, D_o, was $2.00 \pm 0.01 \times 10^5$ cm^2 sec^{-1} for pure D_2O at 20°C compared to an average D_o of $2.10 \pm 0.02 \times 10^5$ cm^2 sec^{-1}

for the static measurements. New pulsed and static measurements in H_2O, as well as in D_2O, have been designed which can be used to test Honeck's calculations.

Deep-poisoned experiments have recently become of interest as a result of theoretical discussions on the limits for which the Boltzmann diffusion equation is formally solvable and on the interpretation of measurements made beyond these limits (Corngold[7]). In the D_2O static experiment a test of one of the formal limits has been accomplished by adding sufficient poison so that κ, the inverse diffusion length, approaches Σ_s, the free atom scattering cross section.

SUMMARY

Pulsed and static experiments were made in H_2O and D_2O to determine diffusion coefficients for these moderators. The experiments included separate investigations of the effects of diffusion cooling, absorption hardening induced by boron poisoning, and neutron source conditions. Spectral indices were measured, in addition to the normal relaxation length and time decay, to determine the magnitude of neutron spectral shifts. The experiments were accompanied by a parallel computational program utilizing Monte Carlo[8] calculations and integral transport calculations by THERMOS.[9]

The SRL H_2O measurements agreed well with the static measurements of Starr and Koppel[10] and with the pulsed measurements of Gon et al.[11] Therefore these three sets of measurements were standardized to σ_B = 759 barns, σ_H = 0.332 barns,[12] and moderator temperature = 20°C. The results of a least squares parametric fit (excepting only the SRL spectral index data) are:

$$D_o = 3.57 \pm 0.04 \times 10^4 \text{ cm}^2 \text{ sec}^{-1}$$

$$C = 3.31 \pm 0.15 \times 10^3 \text{ cm}^4 \text{ sec}^{-1}$$

$$F = 2.8 \pm 0.7 \times 10^2 \text{ cm}^6 \text{ sec}^{-1}$$

These values compare with Honeck's[3] calculations of $D_o = 3.753 \times 10^4$ cm^2 sec^{-1}, $C = 3.130 \times 10^3$ cm^4 sec^{-1}, and $F = 2.700 \times 10^2$ cm^6 sec^{-1}. Spectral index data could not be converted to values comparable to the normal relaxation length measurements because of poor convergence in the P_n theoretical treatment. However, measured and predicted spectral indices in H_2O agreed well.

In D_2O, the SRL pulsed and static measurements agreed with each other and agreed with Honeck's calculations over a limited range of buckling and poisoning values corresponding to an effective Σ_a between -0.04 and +0.04 cm^{-1}. The experimental diffusion coefficients corrected to 20°C and 100 mol % D_2O were:

$$D_o = 2.09 \pm 0.02 \times 10^5 \text{ cm}^2 \text{ sec}^{-1}$$

$$C = 6.6 \pm 0.3 \times 10^5 \text{ cm}^4 \text{ sec}^{-1}$$

These experimental numbers compare with Honeck's[3] calculations of $D_o = 2.072 \times 10^5 \text{ cm}^2 \text{ sec}^{-1}$ and $C = 5.129 \times 10^5 \text{ cm}^4 \text{ sec}^{-1}$.

Our D_2O measurements confirmed Honeck and Michael's results, which showed that the energy spectral shift due to the boron addition should depend on whether a thermal or epithermal neutron source feeds the assembly. We also showed that by properly tailoring the neutron source, a pseudo equilibrium condition could be obtained in heavily poisoned D_2O such that the experimentally assigned value of κ exceeded the theoretical limit of Σ_s (free atom).

DISCUSSION

THEORETICAL DESCRIPTION

The theoretical behavior of the steady-state flux from a distributed neutron source in a diffusing medium has been adequately described.[13] If a source is placed at one end of a sample and if one neglects energy nonequilibrium, the thermal neutron flux is given by an infinite sum of spatial harmonics. For example, if the source is placed on the xy plane at one end of a rectangular parallelopiped with extrapolated dimensions a, b, and c, the neutron flux is given by

$$\phi(x,y,z) = \sum_m \sum_n A_{mn} \sin\left(\frac{m\pi x}{a}\right) \sin\left(\frac{n\pi y}{b}\right) \sinh\left[\gamma_{mn}(c-z)\right] \qquad (1a)$$

where the A_{mn}'s are harmonic amplitude coefficients. The harmonic relaxation lengths γ_{mn} are given by

$$\gamma_{mn}^2 = \kappa^2 + \left(\frac{m\pi}{a}\right)^2 + \left(\frac{n\pi}{b}\right)^2 \equiv \kappa^2 + B_{mn}^2 \ (a,b) \qquad (1b)$$

where

$$\kappa^2 = \frac{\Sigma_a}{D} \qquad (1c)$$

the macroscopic absorption cross section divided by the diffusion coefficient.

The thermal-neutron population of a pulsed medium as a function of time is given by a similar sum. For instance in a cylinder of extrapolated radius R and height H,

$$\phi(r,\theta,z,t) = \sum_\ell \sum_m \sum_n A_{\ell mn} J_m\left(\frac{a_{m\ell} r}{R}\right) \cos(m\theta) \sin\left(\frac{n\pi z}{H}\right) e^{-\lambda_{\ell mn} t} \qquad (2)$$

where $J_m\left(\frac{a_{m\ell} r}{R}\right)$ is a Bessel function of the first kind, $a_{m\ell}$ is

one of the roots of that function, and $\lambda_{\ell mn}$ is the harmonic decay constant of the material.

In both static and pulsed experiments, the fundamental mode (ℓ=m=n=1) is the most persistent, and in principle can be isolated at large z or t values. Honeck has shown the relationship between the fundamental modes in these two experiments.[3] The reciprocal of the diffusion length, κ, in a poisoned moderator at absolute temperature T_o is usually expressed as a function of the poison concentration by the polynomial expansion,

$$\kappa^2 = \alpha_1 \Sigma_a(kT_o) - \alpha_2 \Sigma_a^2(kT_o) + \alpha_3 \Sigma_a^3(kT_o) + \ldots \qquad (3)$$

where k is Boltzmann's constant. Similarly, the fundamental mode decay constant of a pulsed sample is given by the buckling expansion,

$$\lambda = \overline{v\Sigma_2} + D_o B^2 - CB^4 + FB^6 + \ldots \equiv \overline{v\Sigma_a} + (vD_{eff})B^2 \qquad (4)$$

where $\overline{v\Sigma_a}$ is usually written as λ_o for 1/v absorbers.

The identical neutron balance equation describes both experiments in Honeck's time separable treatment when the following identifications are made:

$$\kappa^2 \rightarrow -B^2$$

$$\Sigma_a(kT_o) \rightarrow \frac{\lambda - \lambda_o}{v(kT_o)} \qquad (5)$$

The expansion coefficients of the static experiment are then related to the better known pulsed parameters by the equations,

$$D_o = \frac{v(kT_o)}{\alpha_1}$$

$$C = \frac{v(kT_o)\alpha_2}{\alpha_1^3} \tag{6}$$

$$F = \frac{v(kT_o)(2\alpha_2^2 - \alpha_1\alpha_3)}{\alpha_1^5}$$

The coefficients of Equation 3 may be determined experimentally by measuring κ at several known poison concentrations. Similarly the coefficients of Equation 4 may be determined by measuring the decay constant at several known bucklings.

By noting that only the angular distribution and the neutron temperature effects change D_{eff} when the poison concentration or the sample dimensions are varied, one may then write for a moderator at temperature T_o and neutron temperature T_n;

$$D_{eff} = D(T_o)\left[A + (1-A)\left(\frac{T_n}{T_o}\right)^{\frac{1}{2}}\right](1 + \delta) \tag{7}$$

where it is assumed that the angular distribution and neutron temperature effects are independent. The expression in square brackets is a semiempirical expression[1] for the dependence of D on T_n; at T_o = 293°K, A = 0.69 for D_2O and 0.06 for H_2O. The quantity δ is the angular distribution correction which in the P_3 approximation to monoenergetic transport theory is given closely by

$$\delta(P_3) = \left[\Sigma_a/(5\ \Sigma_{Tr})\right](1 + 4\ \bar{\mu}_o) \qquad \text{Static} \tag{8}$$

$$\delta(P_3) = \left[B^2/(15\ \Sigma_{Tr}^2)\right](1 + 4\ \bar{\mu}_o) \qquad \text{Pulsed} \tag{9}$$

where $\bar{\mu}_o$ is the average cosine of the scattering angle.

Equation 9 was derived explicitly for pulsed systems by Sjostrand.[14] It also follows directly from the application of the equivalence relations of Equation 5 to the well known static relation, Equation 8. The Maxwellian average values of $\bar{\mu}_o$ for H_2O and D_2O have been evaluated by Radkowsky's method[15] in earlier work.[1] At 20°C, $\bar{\mu}_o$ is 0.32 for H_2O and 0.14 for D_2O.

Except for δ, which may readily be evaluated from Equations 8 or 9, D_{eff}, as given by Equation 7, depends only on T_n for a given T_o. Therefore, since the dependence of Σ_a on T_n is trivial, a measurement of T_n alone will give the variation of κ^2 with Σ_a by the relation

$$\kappa^2 = (\Sigma_a)_{eff}/D_{eff} \tag{10}$$

To obtain absolute values of D_{eff} from Equation 7, $D(T_o)$ must be independently determined.

STANDARD EXPERIMENTS

Experimental Methods

The Relaxation Length Measurements

Relaxation length measurements were made in a cadmium-lined Side Tank, a 2-foot cube positioned adjacent to and centered on a 5-foot-square face of the Standard Pile (SP)[16] (Figure 1). A D_2O-filled Slab Tank, 4 inches thick, was interposed between the Side Tank and the SP to increase the thermal-to-epithermal flux ratio in the Side Tank. The neutron flux distribution in the Side Tank was measured by activating bare gold pins, 1/2 inch long and 1/16 inch in diameter, which were placed in holes drilled in a thin-walled aluminum tube extending through the tank. The distance between adjacent pins was either 0.250 or 0.500 inch. Activations due to epithermal source neutrons were subtracted by standard cadmium shutter techniques.

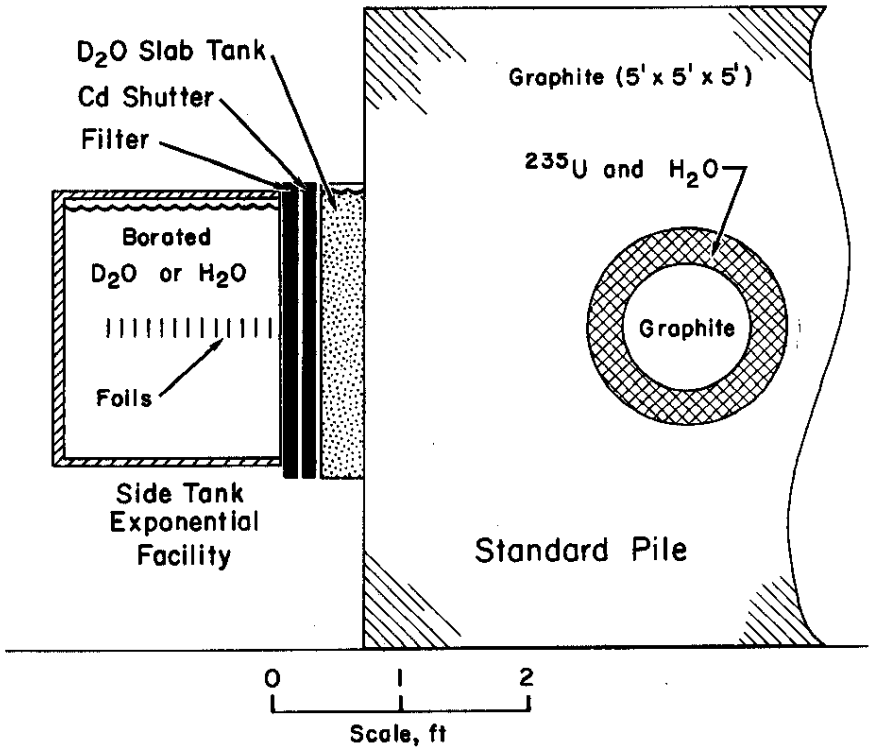

FIG. 1 SOURCE REACTOR AND EXPONENTIAL FACILITY

B_2O_3 was the neutron poison. For H_2O, the highest poison concentration was used first and then diluted successively for lower concentrations. For D_2O, anhydrous B_2O_3 was added in known increments to a fixed amount of D_2O. The absolute boron content of the stock material was determined by mannitol titration and by total dehydration of representative samples in a vacuum oven. The boron isotopic ratio was determined by mass spectrometry. The D_2O purity decreased from 99.84 to 99.78 mol % during the experiment. The added light water from the nominally anhydrous B_2O_3 accounts for 0.026 mol % of this decrease.

The Static Neutron Temperature Experiment

The neutron temperature indices were measured from $\Sigma_a(B)$ = 0 to 0.38 cm^{-1} in the poisoned H_2O, and from $\Sigma_a(B)$ = 0 to 0.06 cm^{-1} in the poisoned D_2O. Lu_2O_3 foils (1/2-inch diameter x 0.020 inch thick, 20 wt % Lu_2O_3 in aluminum matrix) were used as spectral index detectors. In some cases, the lutetium foils were combined with 0.005-inch-thick copper foils into composite foils. The spectral index determination[17] involved the simultaneous irradiation of reference lutetium (and copper) foils in the graphite thermal column of the SP (1/v cadmium ratio $>10^4$) for each sample foil irradiated in the Side Tank. By comparing the ratio of the thermal ^{177}Lu to ^{176}Lu (or ^{64}Cu) activities ratio at the reference to that at test positions, the neutron temperature, T_n, at the sample position was inferred. This temperature was normalized to the moderator temperature, T_o, at the reference position in the graphite, where it was assumed that the thermal neutrons were in temperature equilibrium with the graphite. The light poison experiments were designed to obtain spectral indices for a purely thermal neutron source feeding in from the outside. Since, the available neutron source contained both a thermal and an epithermal component, a cadmium shutter was used to eliminate the effect of epithermal neutrons.

The use of the two lutetium isotopes in single foils was preferred over the combined foils because of the advantage of having identical positions for the two isotopes in the

high-flux gradients. The usual objection to ^{175}Lu as a target atom (a high background due to its high resonance integral) did not apply to most cases because the fluxes were highly thermalized at the foil positions.

The Decay Constant Experiment

The neutron source was a Texas Nuclear double-pulsed, 150 kv accelerator in which deuterons bombard a target containing tritium (Figure 2). Thin-wall aluminum cylinders of the dimensions listed in Table I contained samples of 99.84 mol % D_2O or deionized H_2O; the sample heights were known within ±0.02 cm. In the two largest cylinders, cadmium sheets were inserted on the underside of the cover plate to eliminate backscattering from the plate;[18] however, no discernible difference was observed without the cadmium. Targets were placed on the vertical axis of the samples with 6 inches of bottom clearance. D_2O was transferred by dried helium gas under pressure. The helium also minimized isotopic degradation.

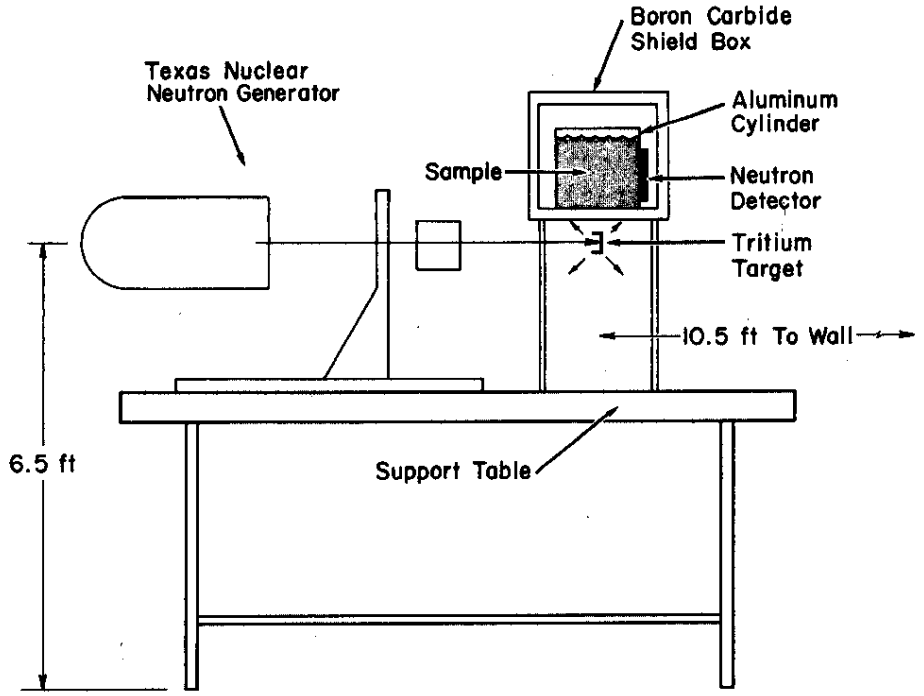

FIG. 2 NEUTRON GENERATOR, SAMPLE, AND SHIELD BOX

TABLE I

Dimensions of Aluminum Cylinders Used for Pulsed Measurements

(All cylinders have a nominal 20-in. inner height)

Radius	Side Wall Thickness	Bottom Wall Thickness
	(All dimensions in inches)	
11.873	0.125	0.250
5.886	0.125	0.250
3.894	0.100	0.125
2.929	0.061	0.125
1.955	0.040	0.125

The neutron detector was placed on the bottom axis of the sample or at the half-height on the side. The detector was either an assembly of 10 decoupled counters (N. C. Wood) filled with 0.4 atm of $^{10}BF_3$ or a single counter (Texas Nuclear) filled with 10 atm of ^{3}He. Counts were stored in 100 equally spaced time channels of a multichannel analyzer (RIDL 34-12B) with at least 30 of the final channels at the background level.

A computer code (PEX[19]) based on Peierls' statistical method[20] was used to determine the decay constant from the measured decays. This code features the use of the centroid rather than the midpoint of each counting interval, and the following choice of methods for eliminating background: if dark current is the only contributor, the code subtracts a constant value; if a background varies slowly compared to the desired counts, the code takes the difference between adjacent channels as the desired count, or takes the difference, by channel, between successive runs in which only the source-to-sample distance is varied. This last method is based on the condition common to most pulsed experiments -- the desired counts are strongly sensitive to the source-to-sample distance whereas the background of wall-return neutrons is nearly independent of this distance.

The deadtime of the recording system with a single BF_3 counter was determined by the two-source technique to be considerably higher than that obtained with a double pulser for the electronics alone. Combining uncoupled BF_3 counters enabled

the system deadtime to approach the electronic deadtime of 1.7 μsec. A deadtime correction based on the appropriate two-source value was included in the analytical code.

The most serious problem faced in the experiment was wall return of epithermal neutrons. These neutrons are thermalized slowly because of the finite transit times in the room. If intercepted in the sample, they extend the decay and thus lower the λ assignment. To minimize the effect, all experiments were performed inside a cadmium-lined box with 2-inch-thick walls of compacted B_4C (Figure 2). Small sample experiments were performed in a relatively large room (6.5 feet to the floor and 10.5 feet to nearest wall), and the two-position technique was used.

Special care was taken to minimize spatial harmonics. The angular component can be eliminated by placing the neutron source on the axis of the sample. Similarly, the first axial harmonic can be eliminated by placing the detector at the midplane. The degree of harmonic contribution also depends on the sample shape; the relative difference in the fundamental decay constant and that of the nearest harmonic is greatest when sample dimensions are nearly equal, i.e., harmonic contributions disappear fastest in regular geometries. Spherical shapes are ideal but are difficult to fabricate; as a compromise, graduated cylinders were used. The incomplete elimination of source harmonics (and incomplete thermalization as well) can be detected by noting the variation of the derived decay constant with the starting channel for a given set of data.

The Pulsed Neutron Temperature Experiment

The experimental technique was similar to that used in neutron total cross section studies[21] (Figure 3). Two BF_3 counters are wrapped in cadmium except for one end which opened into cadmium-collimated re-entry tubes in the pulsed medium. Only neutrons originating from near the ends of re-entry tubes (placed in symmetric locations in a given sample) can pass

through the neutron collimators. Two separate "detector-dependent" transmissions, Tr_A and Tr_B,[22] are measured as functions of time by: placing a gold foil between the collimator and the detector of Unit A while Unit B is left open; pulsing the sample and observing the neutron die away in both counters; and then repeating with the foil moved to Unit B while Unit A is opened. Any effects of unbalanced counter efficiencies or of geometric asymmetries are automatically canceled by using the geometric mean for the reported transmission, $Tr = (Tr_A\ Tr_B)^{\frac{1}{2}}$.

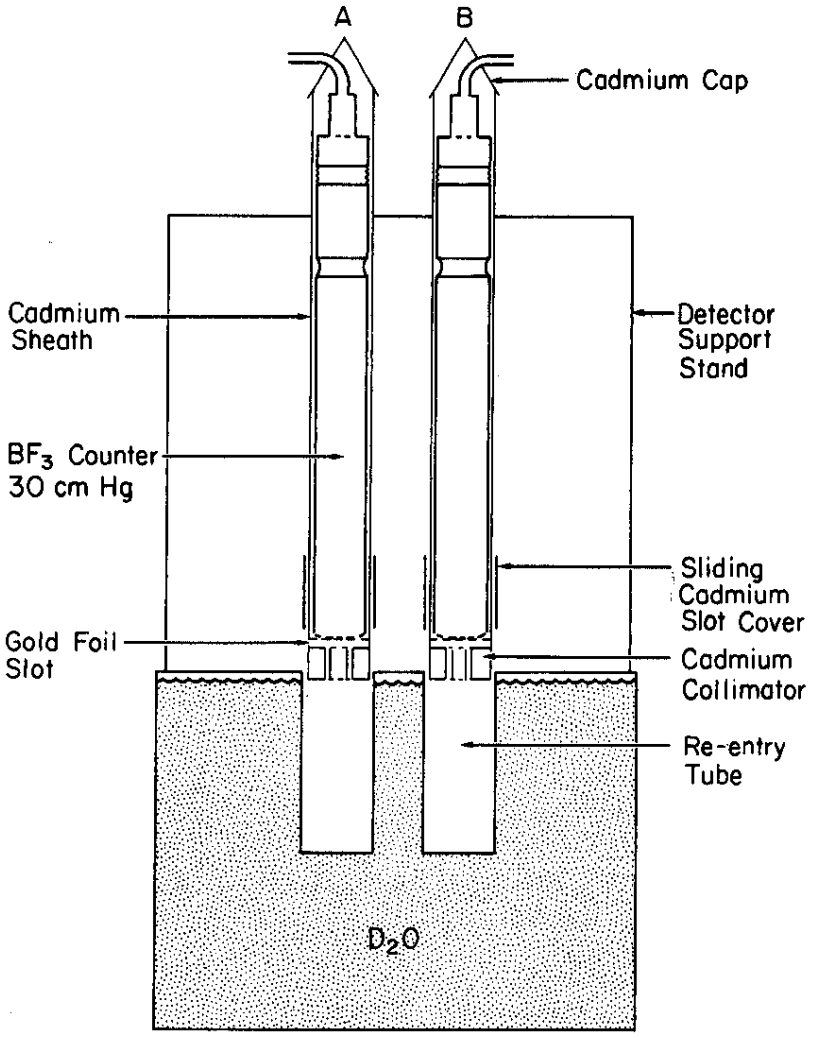

FIG. 3 PULSED NEUTRON TEMPERATURE EXPERIMENT

These transmissions were converted to neutron temperatures by a calibration at identical pulsed conditions with the re-entry tubes inserted into a paraffin sample at 295, 196, and 77°K. The calibration sample was large enough so that diffusion cooling was negligible. The neutron spectrum measured is that of the equilibrium, or asymptotic, condition and coincides with that measured by time-of-flight methods using double-gating techniques.[23]

Analysis of H_2O Data

Relaxation length measurements in poisoned H_2O are summarized in Table II. The fundamental transverse buckling correction, $B_{11}^2(a,b)$ of Equation 1b, was less than 5% of κ^2 for all static H_2O experiments; thus the effect of higher harmonics was small and was eliminated in least squares fits by successive dropping of data points near the source face.

The neutron temperature measurements on H_2O are also tabulated in Table II. The $R^{Lu}/R^{1/v}$ ratios are:

$$R^{Lu}/R^{1/v} = \frac{(^{177}\text{Lu Act.})^{Test}/(^{177}\text{Lu Act.})^{Ref.}}{(\ 1/v\ \text{Act.})^{Test}/(\ 1/v\ \text{Act.})^{Ref.}} \qquad (11)$$

where the subcadmium activations in the test medium are normalized to the subcadmium activations in the thermal reference flux. Simultaneous irradiation and intermixing of foils on a single counting system allow the ratios of Equation 11 to be used with no correction.

The two pulsed measurements in H_2O (Table II) were made primarily to check against Gon's[11] measurements. Because of Gon's use of spherical geometry and an inherently effective method of handling wall-return neutrons, we considered the excellent agreement between our data and his (Figure 4) to be a sufficient check of our method.

TABLE II

Static and Pulsed Measurements in H_2O

Inverse Diffusion Lengths and Neutron Temperatures in Borated H_2O at 22°C

	Diffusion Length		Neutron Temperature			
$\Sigma_a(B)$, cm^{-1}	κ^2, cm^{-2}	$\frac{\kappa^2}{\Sigma_a(B) + \Sigma_a(H_2O)}$, cm^{-1}	Distance in Tank, in.	$R^{Lu}/R^{1/v}$	T_n/T_o	$\frac{\kappa^2}{\Sigma_a(B) + \Sigma_a(H_2O)}$, cm^{-1} (a)
0	0.136 ±0.002	6.10 ±0.08	2.0	1.00	1.00 ±0.01	6.06 ±0.08(b)
0.00601 ±0.00003	0.169 ±0.002	5.99 ±0.08	-	-	-	-
0.01200 ±0.00006	0.206 ±0.003	6.03 ±0.08	-	-	-	-
0.0239 ±0.0001	0.276 ±0.003	6.00 ±0.08	-	-	-	-
0.0480 ±0.0002	0.417 ±0.005	5.95 ±0.08	1.5	1.06	1.05 ±0.01	5.90 ±0.08
0.0960 ±0.0005	0.694 ±0.009	5.87 ±0.08	1.5	1.11	1.09 ±0.02	5.73 ±0.10
0.0960 ±0.0005	0.690 ±0.009	5.84 ±0.08	1.5	1.09	1.07 ±0.02	5.83 ±0.10
0.1539 ±0.0008	0.994 ±0.013	5.64 ±0.08	1.5	1.10	1.08 ±0.02	5.86 ±0.10
0.205 ±0.001	1.23 ±0.02	5.41 ±0.08	1.0	1.21	1.17 ±0.03	5.47 ±0.12
0.272 ±0.001	1.56 ±0.02	5.29 ±0.08	1.0	1.24	1.20 ±0.03	5.41 ±0.12
0.272 ±0.001	1.54 ±0.02	5.22 ±0.08	1.0	1.20	1.16 ±0.03	5.61 ±0.12
0.361 ±0.002	1.98 ±0.03	5.17 ±0.08	1.0	1.29	1.24 ±0.03	5.35 ±0.12

Pulsed Decay Constants in H_2O at 24.6°C

Sample	Radius, in.	Height, in.	Counter and Position	Convergence Time to Asymptotic Decay, μsec	Uncorrected Decay Constant, 10^3 sec^{-1}	Final Buckling, cm^{-2}	$\kappa^2/\Sigma_a(20°C)$, cm^{-1}
1	3.894	6.020	BF_3 side	600	8.30 ±0.03	0.09470	6.13 ±0.03
2	1.955	3.930	BF_3 side	450	15.24 ±0.08	0.29722	6.40 ±0.05

(a) P_3 Approximation, Equation 8.

(b) Normalized at $\Sigma_a(B) = 0$ to the least squares fit of the relaxation length data.

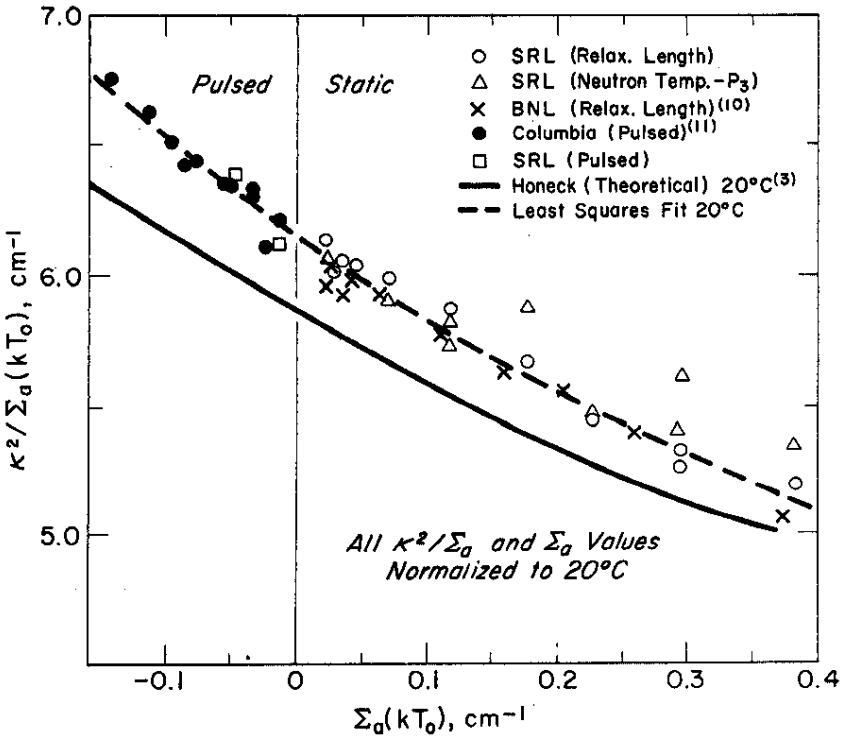

FIG. 4 COMPARISON OF EXPERIMENTAL DATA TO THEORETICAL CALCULATIONS FOR H_2O (T_o = moderator temperature = 20°C)

All SRL data along with Starr and Koppel's (BNL) static data[10] and Gon's (Columbia) pulsed data are shown in Figure 4. The BNL data have been recomputed using a best value[12] of 0.332 barns for the absorption cross section of hydrogen and 759 barns for boron. (It is believed that the hydrogen cross section is known far more accurately than it can be derived from a single experiment of this nature.) The static results of Bretscher and Meyer,[24] although not shown on Figure 4, agree with our measurements and the BNL results, but are more scattered.

To display the static spectral index measurements on Figure 4, they had first to be converted to neutron temperatures.[17] These temperatures were then used to derive κ^2 from Equation 10. Equations 7 and 8 were used to evaluate D_{eff} with the result at $\Sigma_a(B) = 0$ normalized to the experimental curve in Figure 4. If the P_1 approximation instead of P_3 had been used, the spectral index data in Figure 4 would have been more consistent.

The combined pulsed and static data in Figure 4 deviated from Honeck's calculations in the zero poison intercept. The slope, however, has been closely predicted. All the data in Figure 4 except the spectral index data have been used in a three-parameter least squares fit to Equation 3. The best fit parameters at a temperature of 20°C are:

$$\alpha_1 = 6.155 \text{ cm}^{-1}$$

$$\alpha_2 = 3.51$$

$$\alpha_3 = 2.2 \text{ cm}^{+1}$$

These transform to the usual pulsed parameters:

$$D_o = 3.57 \pm 0.04 \times 10^4 \text{ cm}^2 \text{ sec}^{-1}$$

$$C = 3.31 \pm 0.15 \times 10^3 \text{ cm}^4 \text{ sec}^{-1}$$

$$F = 2.8 \pm 0.7 \times 10^2 \text{ cm}^6 \text{ sec}^{-1}$$

Systematic errors which may be present in cross section assignments are not included in the above error bars.

Analysis of D_2O Data

Relaxation length measurements in light-to-intermediate poisoned D_2O are summarized in Table III and in heavily poisoned D_2O in Table V. For D_2O, the effect of higher order harmonics was large; therefore, harmonic amplitude coefficients (the A_{mn} of Equation 1) had to be determined. A set of coefficients was determined by fitting Equation 1 to the unpoisoned flux distributions using the previously measured[1] value of $\kappa(0)$. A three-parameter fit for the three dominant amplitudes, A_{11}, $A_{13} = A_{31}$, and $A_{15} = A_{51}$, was determined. These derived amplitudes were used to eliminate the harmonic content of the measured data. The resulting κ values of the intermediate poisoned samples agree well with those derived by successive dropping

of data points. In heavily poisoned D_2O, the dependence on $\kappa(0)$ becomes small, and for $\Sigma_a > 0.05$ cm^{-1}, variations as large as 5% in the assumed reference value affected the quoted κ^2 only slightly.

TABLE III

Inverse Diffusion Lengths and Neutron Temperatures in Borated D_2O

				Diffusion Length			Neutron Temperature				
$\Sigma_a(B)$, cm^{-1}	D_2O Purity, mol %	Sample Temp, °C	κ^2, cm^{-2}	$\frac{\kappa^2}{\Sigma_a(B) + \Sigma_a(D_2O)}$, cm^{-1}		Distance in Tank, in.	$R^{Lu}/R^{1/v}$	T_n/T_o	$T_{n(\infty)}/T_o$ [b]	$\frac{\kappa^2}{\Sigma_a(B) + \Sigma_a(D_2O)}$ [c], cm^{-1}
0	99.84	22.0	0.000083 [a]	1.049 [a]		12	0.99	0.99	0.99 ±0.01	1.06 ±0.01
0.00583 ±0.00004	99.84	22.1	0.00604 ±0.00011	1.04	±0.02	12	0.99	0.99	0.99 ±0.01	1.06 ±0.01
0.0142 ±0.0001	99.84	22.5	0.0144 ±0.0003	1.02	±0.02	6.3	1.12	1.10	1.10 ±0.02	1.01 ±0.01
0.0230 ±0.0002	99.83	22.8	0.0228 ±0.0005	0.99	±0.02	4.8	1.13	1.11	1.11 ±0.02	1.00 ±0.01
0.0401 ±0.0003	99.83	22.1	0.0378 ±0.0008	0.94	±0.02	6.3	1.18	1.15	1.15 ±0.02	.99 ±0.01
0.0583 ±0.0004	99.82	22.5	0.0556 ±0.0012	0.95	±0.02	3.2	1.25	1.21	1.22 ±0.03	.97 ±0.02

(a) Reference (1)

(b) Corrected to Asymptotic Value

(c) P_3 Approximation, Equation 8.

Axial activation profiles are plotted in Figure 5 for a nonpoisoned, a lightly poisoned, and the three most heavily poisoned D_2O samples. These are shown as ratios of measured-to-analytic fitted activities. The harmonic correction is that required to systematize the data for $\Sigma_a(B) = 0$ and 0.023 cm^{-1}. The data for heavily poisoned D_2O is discussed in a later section.

To obtain the relaxation times from the pulsed measurements and the geometrical bucklings, special analytical techniques were required since in D_2O the magnitude of the extrapolation distance is significant. In determining the extrapolation distances, the reflection effect of the aluminum walls, changes

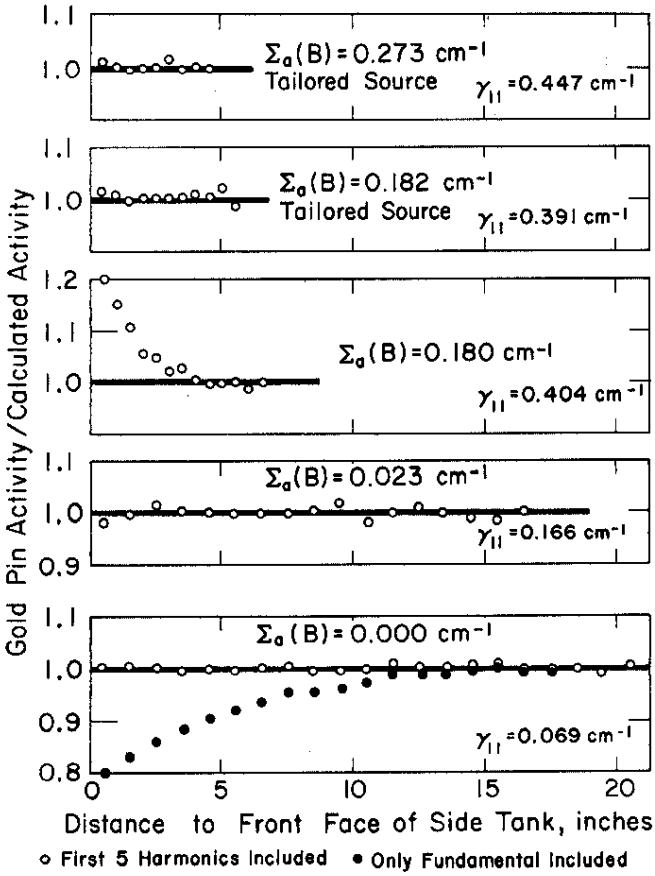

FIG. 5 APPROACH TO EQUILIBRIUM IN RELAXATION LENGTH MEASUREMENTS ON BORATED D_2O

in radial extrapolations due to curvature of the walls,[25] and the change of transport mean free path with sample size due to spectral cooling were included. Small changes in temperature and moderator purity during the experiment were also corrected for. Our expression for the radial extrapolation distance in terms of the slab distance was taken from Flatt and Baller.[25] The extrapolation distance is estimated initially to compute $\frac{\lambda-\lambda_o}{B^2}$. This is then identified as $(vD)_{eff}$, and the computation is iterated with the new extrapolation distance which can be obtained from the extraction of D_{eff}. The iterative procedure is detailed in the Appendix. Two neutron temperature determinations were also made by pulsed methods. These data and all the relaxation time measurements are listed in Table IV.

TABLE IV

Pulsed Measurements in D_2O

Pulsed Decay Constants in D_2O

Sample	Radius, in.	Height, in.	Moderator Temp, °C	Counter and Position	Convergence Time to Asymptotic Decay, μsec	Uncorrected Decay Constant, 10^3 sec^{-1}	Final Buckling, cm^{-2}	Normalized to 29°C and 99.84 mol %: Σ_a, cm^{-1}	Normalized to 29°C and 99.84 mol %: κ^2/Σ_a, cm^{-1}
1	11.873	16.075	27.6	BF_3 side	2000	2.158 ±0.004	0.01062	-0.0098	1.082 ±0.003
2	11.873	12.147	27.6	BF_3 side	1500	2.805 +0.007	0.01392	-0.0127	1.096 ±0.005
3	11.873	9.103	27.9	BF_3 side	900	3.845 ±0.007	0.01941	-0.0174	1.113 ±0.002
4	5.886	16.105	29.5	BF_3 side	700	5.00 ±0.01	0.02577	-0.0226	1.139 ±0.002
5	11.873	6.028	28.2	BF_3 side	550	6.11 ±0.02	0.03321	-0.0277	1.197 ±0.004
6	5.886	6.028	29.0	BF_3 side	400	8.74 ±0.05	0.04869	-0.0397	1.228 ±0.007
7	3.894	10.047	28.2	BF_3 side	500	9.42 ±0.01	0.05532	-0.0428	1.293 ±0.002
8	5.886	5.024	23.4	^3He bottom	550	10.16 ±0.10	0.06300	-0.0481	1.31 ±0.01
9	3.894	6.018	29.4	BF_3 side	350	11.66 ±0.05	0.07195	-0.0529	1.360 ±0.006
10	2.929	10.057	23.2	^3He bottom	400	12.7 ±0.3	0.08300	-0.0579	1.43 ±0.03
11	3.894	4.029	23.1	BF_3 side ^3He bottom	350	14.37 ±0.05	0.09711	-0.0654	1.485 ±0.005
12	2.929	5.024	23.3	^3He bottom	300	15.4 ±0.3	0.11070	-0.0708	1.56 ±0.03
13	3.894	3.014	23.0	^3He bottom	300	16.7 ±0.8	0.12714	-0.0766	1.66 ±0.08
14	1.955	16.075	23.7	^3He side	250	19.2 ±0.3	0.14891	-0.0881	1.69 ±0.03
15	1.955	6.028	22.9	^3He side	250	20.7 ±1.1	0.17295	-0.0953	1.82 ±0.10
16	3.894	2.009	23.0	^3He bottom	250	21.9 ±0.6	0.18991	-0.1008	1.89 ±0.05
17	1.955	4.019	23.0	^3He bottom	200	24.1 ±1.5	0.20082	-0.1109	1.81 ±0.11

Pulsed Neutron Temperatures in D_2O at 24.7°C

Sample	Radius, in.	Height, in.	Decay Constant for Buckling Estimate, X 10^3 sec^{-1}	Final Buckling, cm^{-2}	Neutron Temp, °K	Normalized to 29°C and 99.84 mol %: Σ_a, cm^{-1}	Normalized to 29°C and 99.84 mol %: κ^2/Σ_a, cm^{-1} [a]
1	5.886	8.0	6.86	0.0370	235 ±8	-0.0312	1.19 ±0.03
2	3.894	6.0	11.55	0.0715	188 ±6	-0.0525	1.34 ±0.02

(a) P_3 Approximation, Equation 9.

The combined, but unnormalized, pulsed and static data in Figure 6 agree reasonably well with Honeck's calculations[3] over a restricted range near the origin. The cause of disagreement with theory at small pulsed samples (large negative absorption cross sections) is not clear. The data may disagree because Honeck's pulsed computations were actually static computations transformed by the equivalence relations, Equations 5 and 6; the range of validity of Equation 6 may be severely limited. Also, since the pulsed neutron temperature measurements agree better with experimental decay times than with theory, the disagreement may arise because the theory failed to properly predict the neutron spectrum. Recently Ghatak and Honeck[26] made a series of computations for graphite in which the neutron density was treated as a nonseparable function of time and energy. The resultant values of κ^2/Σ_a at high bucklings were larger than those found in previous energy-independent studies and agreed better with the data of Starr and Price.[27] A similar calculation for D_2O could have the same effect. Still another cause for disagreement might be that the pulsed data asymptotically approached a possible Corngold $\lambda = (v\Sigma_t)_{min}$ limit, which is depicted in Figure 6.

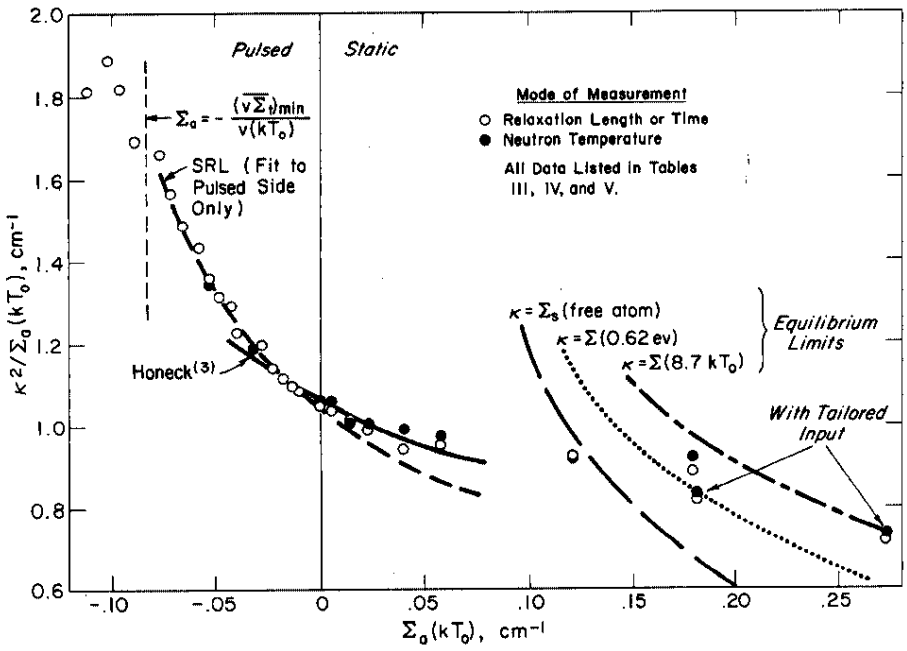

FIG. 6 COMPARISON OF EXPERIMENTAL DATA TO THEORETICAL CALCULATIONS FOR D_2O (T_o = moderator temperature as listed in Tables III, IV, and V)

It did not seem that systematic errors would explain the discrepancy. The pulsed results could have been erroneous had an asymptotic energy equilibrium not been reached. However, the direction of the required correction is such that the disagreement between experiment and theory increases. Moreover, correcting for a possible failure to reach spatial equilibrium would only remove the internal consistency of the data. Our experience shows the discrepancy may also result from failure to have completely eliminated wall-return neutrons. However, in the H_2O work, where wall return was particularly evident, our results agreed quite well with the data of Gon et al.,[11] who by the unique design of their experiment should have eliminated practically all wall return.

If a weighted least squares analysis is performed on all our normalized pulsed data with only the experimental errors in the λ measurements being considered, the diffusion parameters at 29.0°C and 99.84 mol % D_2O are:

$$D_o = 2.12 \pm 0.02 \times 10^5 \text{ cm}^2 \text{ sec}^{-1}$$

$$C = 8.1 \pm 0.3 \times 10^5 \text{ cm}^4 \text{ sec}^{-1}$$

$$F = 16 \pm 4 \times 10^5 \text{ cm}^6 \text{ sec}^{-1}$$

In Figure 6 this fit is indicated by a dashed line; however, an extension into the static region indicates that these parameters are not adequate. Since we should avoid using data that approaches either the pulsed or static Corngold limits, we have used data between $\Sigma_a = -0.04$ and $+0.04$ cm^{-1} for extracting the best parametric fit to the combined pulsed and static data. Pulsed and static data were normalized to 29°C using Equation 7. These normalized data and least squares fit are shown in Figure 7; the best fit parameters at 99.84 mol % D_2O and 29°C are:

$$\alpha_1 = 1.054 \text{ cm}^{-1}$$

$$\alpha_2 = 3.42$$

$$\alpha_3 = 29.1 \text{ cm}^{+1}$$

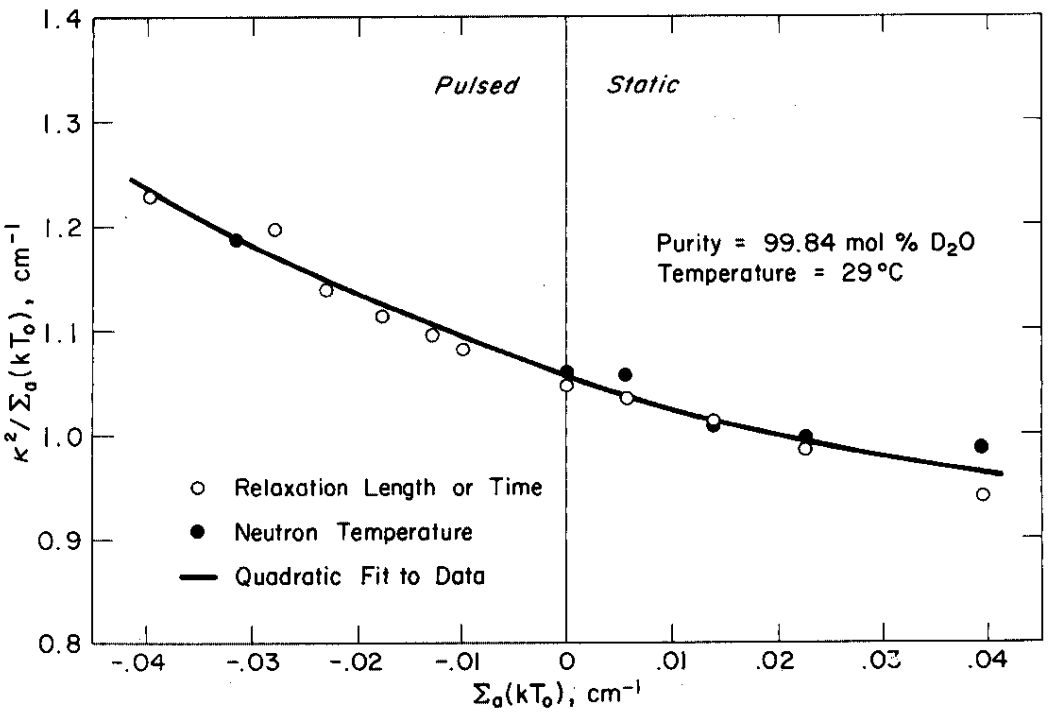

FIG. 7 RESTRICTED RANGE EXPERIMENTAL DATA IN D_2O
(T_o = moderator temperature = 29°C)

These transform to the usual pulsed parameters:

$$D_o = 2.12 \pm 0.02 \times 10^5 \text{ cm}^2 \text{ sec}^{-1}$$

$$C = 6.5 \pm 0.3 \times 10^5 \text{ cm}^4 \text{ sec}^{-1}$$

$$F = -13 \pm 10 \times 10^5 \text{ cm}^6 \text{ sec}^{-1}$$

We have corrected these coefficients to 100 mol % D_2O and 20°C. While the D_o correction is straightforward, the C correction is uncertain. We have used the computations of Honeck and Michael[2] for the temperature variation of C and Paulk's[28] experimental data for the isotopic purity correction. The obviously poorly determined F was not corrected. Our final normalized values at 100 mol % D_2O and 20°C are:

$$D_o = 2.09 \pm 0.02 \times 10^5 \text{ cm}^2 \text{ sec}^{-1}$$

$$C = 6.6 \pm 0.3 \times 10^5 \text{ cm}^4 \text{ sec}^{-1}$$

SPECIAL STATIC EXPERIMENTS

Dependence on Source Conditions in H_2O

For H_2O the term $4\bar{\mu}_o$ in Equation 8 is greater than unity, and the P_n series approximation does not converge rapidly. Thus substituting Equation 8 into Equation 7 does not give a satisfactory expression for the dependence of κ on neutron temperature; thus calculated and experimental neutron spectra should be compared directly. Such a comparison is shown in Figure 8. In the Monte Carlo calculations,[8] Brown's temperatures[29] are used which were obtained by least square fitting a Maxwellian distribution. The THERMOS[9] temperature ratios are proportional to $\bar{v}^2$, the square of the neutron velocities averaged over the neutron density in the energy interval 0 to 0.14 ev. Figure 8 clearly shows that source conditions do not strongly affect the calculated spectral shifts. The following paragraphs show that the experimental data, if properly interpreted, support the theoretical results.

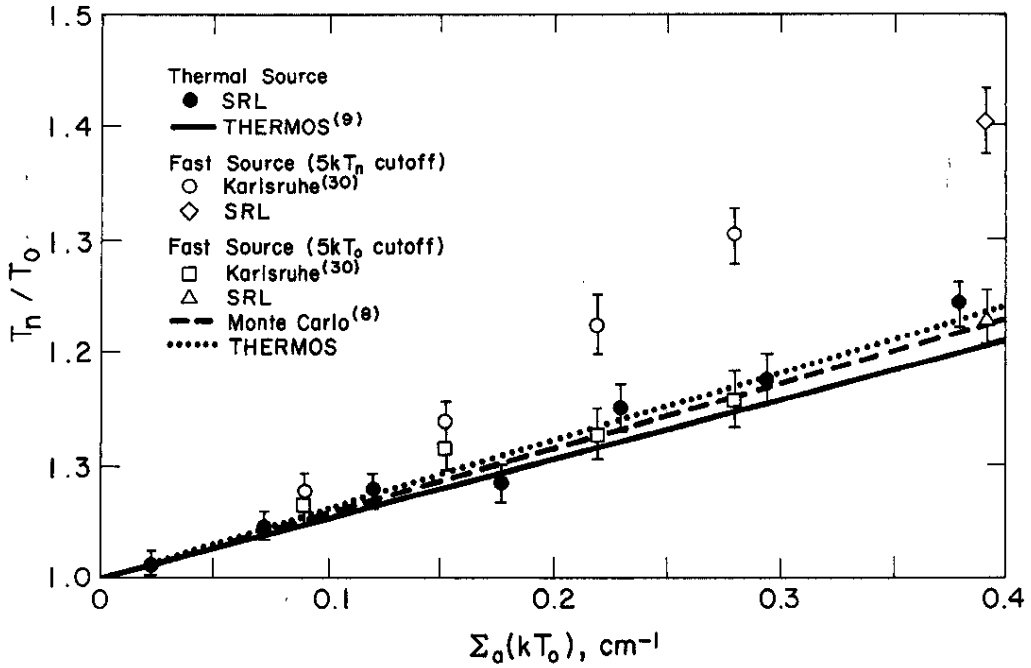

FIG. 8 COMPARISON OF ASYMPTOTIC NEUTRON TEMPERATURES DERIVED FROM SPECTRAL INDEX MEASUREMENTS AND THEORETICAL CALCULATIONS FOR H_2O

During the course of our experiments, similar activation temperature measurements were also being made at Karlsruhe by Burkart.[30] The neutron temperature ratios derived by Burkart are shown in Figure 8 as the open circles. His absorption hardened temperatures are nearly a factor of two higher than those measured at SRL. In attempting to reconcile this discrepancy, experimental differences were noted between the SRL and Karlsruhe studies. The SRL source was essentially a thermal neutron source, the neutrons being supplied by diffusion. In contrast, the low cadmium ratios reported by Burkart indicate a very high epithermal component, in fact, indistinguishable from that for a multiplying medium[31] having the same thermal neutron absorption cross sections. Further, Burkart used cadmium pillboxes rather than a shutter for the epithermal correction. As a test of Burkart's data, a single measurement was made at SRL on a heavily poisoned H_2O sample fed by a pure slowing-down source, which was obtained by covering a 4-inch-diameter cylinder with cadmium and irradiating it in a mixed fast-thermal flux. Bare and cadmium-covered (pillbox) lutetium and copper foils were placed along the axis of the cylinder. As shown in Figure 8, the data point, ◇, from this experiment fits smoothly onto Burkart's data. The measured cadmium ratio also fits a linear extension of his data.

In correcting for the effect of epithermal neutrons, Burkart used Westcott's method[32] and the derived neutron temperature, T_n, to determine the cutoff energy separating the thermal flux from the 1/E epithermal flux. Because absorption hardening only depletes the low energy end of the distribution, the use of this increased cutoff energy is questionable. If Burkart's data are reanalyzed using T_o rather than T_n, the derived neutron temperatures are strongly reduced and, as shown in Figure 8, they then lie somewhat below those measured at SRL.

Our interpretation is further supported by THERMOS computations for the $\Sigma_a(B) = 0.371\ cm^{-1}$ entry in Table V. The calculation gives the same neutron temperature ratio, $T_n/T_o = 1.23$, as given by the Wescott analysis using T_o for the cutoff,

TABLE V

Special Static Experiments

			Diffusion Length		Neutron Temperature				
Σ_a(B)	D_2O Purity, mol %	Sample Temp, cm^{-2}	κ^2 cm^{-2}	$\frac{\kappa^2}{\Sigma_a(\text{total})}$, cm^{-1}	Distance in Tank, in.	$R^{Lu}/R^{1/v}$	T_n/T_o	$T_{n(\infty)}/T_o$	$\frac{\kappa^2\ (a)}{\Sigma_a(\text{total})}$, cm^{-1}
				Fast Source in H_2O					
0.371	-	-	-	-	2.0	1.52	1.40 ±0.02(b) 1.23 ±0.02(c)		
				Fast Source in D_2O					
0.045	99.83	-	-	-	2.0	1.68	1.30 ±0.03		
				Heavily Poisoned D_2O					
0.121(d)	99.80	23.6	0.1116	0.924	2.1	1.41	1.34	1.44 ±0.04	0.92 ±0.02
0.180(d)	99.78	-	0.1589	0.883	2.3	1.42	1.36	1.51 ±0.05	0.92 ±0.02
0.182(e)	99.72	26.5	0.1480	0.813	2.4	1.82	-	1.74 ±0.02	0.83 ±0.02
0.273(e)	99.68	31.5	0.1950	0.715	2.4	2.20	-	2.25 ±0.10	0.74 ±0.03

(a) P_3 Approximation, Equation 8.

(b) T_n Cutoff

(c) T_o Cutoff

(d) Thermal Source

(e) Tailored Source

and also predicts a value of R = 1.47, within 3% of the measured subcadmium activation ratio.

Dependence on Source Conditions in D_2O

The strong dependence of the neutron spectrum on the source feed for poisoned D_2O is shown in Figure 9. This figure shows Monte Carlo computations[33] and THERMOS computations for poisoned D_2O with fast and thermal sources. In the THERMOS computations, the thermal source condition was obtained by a multiregion computation having a source-free poisoned region. As with H_2O, the two computational methods agree closely but, unlike the H_2O case, both methods now show a marked dependence on the source feed.

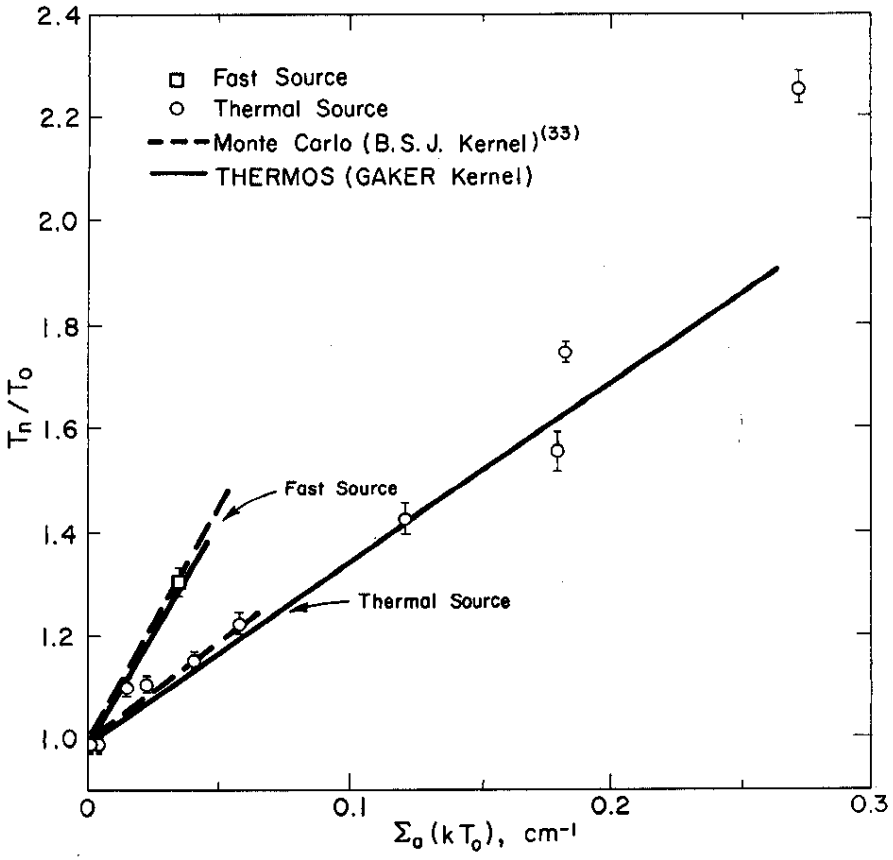

FIG. 9 COMPARISON OF ASYMPTOTIC NEUTRON TEMPERATURES DERIVED FROM SPECTRAL INDEX MEASUREMENTS AND THEORETICAL CALCULATIONS FOR D_2O

The neutron temperature ratios derived from the lutetium activations agree reasonably well with the computed temperature ratios over the entire range. The intermediate ratios include THERMOS computed corrections to the measured ratios to account for the nonasymptotic energy distribution at the foil position. These corrections are the differences between the $T_{n(\infty)}/T_o$ and T_n/T_o columns of Table III.

A single measurement with an epithermal energy feed was made in the small 4-inch-diameter cadmium-covered container at $\Sigma_a = 0.0450\ cm^{-1}$. Interpreting the measured activation ratios as neutron temperatures by the Westcott method failed completely because the method was inadequate to treat the spectrum in the 0.1 to 0.6 ev energy interval. Instead, the neutron temperature is inferred from the measurements by THERMOS computations. This is accomplished by first finding an absorption cross section such that the THERMOS predicted activation ratio for the small sample matches that of the experiment as listed in Table V. This same cross section is used in a second computation that assumes no leakage. The neutron temperature for the infinite case is then determined from the average neutron velocity given by the second computation. The temperature thus derived from the measurement is (Figure 9) consistent with both of the depicted computational methods.

A Test of the Theoretical Equilibrium Limit in D_2O

The most heavily poisoned cases ($\Sigma_a > 0.12\ cm^{-1}$) are particularly interesting since a formal equilibrium limit for the solution of the Boltzmann equation is either approached or exceeded.[7] In the past, this limit has been interpreted to mean that higher asymptotic values of κ could not be obtained experimentally. In an effort to examine this region, we performed tests at three poison concentrations. (All data for these heavily poisoned D_2O samples are listed in Table V and displayed in Figures 5, 6, 9, and 10.) The data points at $\Sigma_a = 0.273\ cm^{-1}$ were obtained only with a tailored incident spectrum closely matching the equilibrium distribution. This spectrum was supplied by heating the 4-inch Slab Tank to 90°C and inserting between

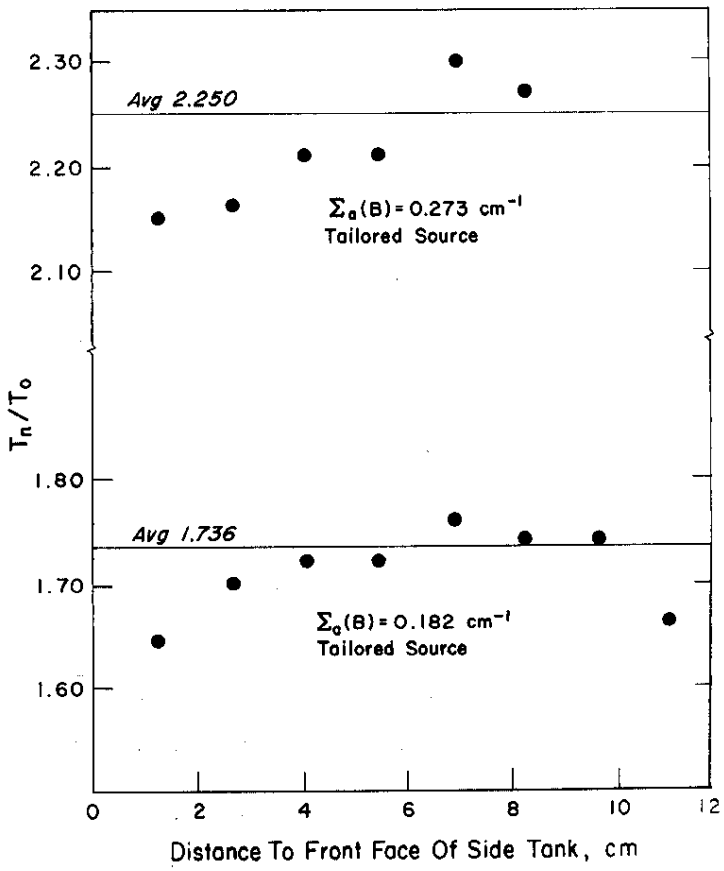

FIG. 10 NEUTRON TEMPERATURES DERIVED FROM SPECTRAL INDEX MEASUREMENTS IN HEAVILY POISONED D_2O VERSUS DISTANCE INTO EXPONENTIAL FACILITY

the Slab and Side Tanks sheets of boron-steel alloy that had a thermal neutron absorption thickness of 2.0 mean free paths (Figure 1). The spectral index measurements as a function of distance into the poisoned D_2O (Figure 10) varied only slightly. Furthermore, the activation measurement at $\Sigma_a(B) = 0.273\ cm^{-1}$, shown at the top of Figure 5, does not depart from simple exponential behavior over the entire experimental range.

The data points at the poison concentration around $\Sigma_a = 0.18\ cm^{-1}$ were obtained with and without tailoring. At $\Sigma_a = 0.182\ cm^{-1}$ the tailored spectrum was supplied by heating the 4-inch Slab Tank to 90°C and inserting a filter with a 1.0 mean free path thickness. Energy equilibrium again appeared to be established as seen in Figure 10. In contrast, at $\Sigma_a = 0.180$

cm^{-1}, where the incident spectrum from the SP was unaltered, energy equilibrium was never established within the experimental region, although the axial flux profile shown in Figure 5 seems to be exponential over half its range. THERMOS computations were also made for this case to correct the spectral measurements to the asymptotic case, but as seen in Figures 6 and 9 even this correction did not make the spectra agree completely with spectra obtained with the tailored source. Since this same correction technique was used for $\Sigma_a = 0.121\ cm^{-1}$ which was irradiated with an untailored source, we might expect this value of $T_{n(\infty)}/T_o$ to be too low.

As seen in Figure 6, the measurements on D_2O were not seemingly influenced by the $\kappa = (\Sigma_s)_{min}$ limit. Corngold and Michael[34] have commented about relaxation length measurements on beryllium which seemingly violate this same limit, except that the limit is here imposed at low energies by Bragg scattering. Analogous violations of similar theoretical limits have also been noted for pulsed measurements on crystalline moderators. Corngold and Durgun[35] have recently given an interpretation of these measurements.

For the D_2O static measurements, a simple qualitative explanation of the role of this limit may be given. The thermal neutron source feeding the assembly is a Maxwellian distribution. In any energy interval, the flux at that energy can fall off with distance no more rapidly than the rate at which neutrons are removed from this energy interval by capture or by scattering collisions to other energies. Thus, at very large distances from the source, the spatial variation of the measured activation profile must be determined by neutrons in the energy interval for which the removal cross section is a minimum, unless the energy average diffusion length for the Maxwellian distribution is long enough to exceed such "removal lengths" (inverse total macroscopic cross sections) at all energies. Since Maxwellian distributions formally extend to infinite energies, energies up to infinity should be included. It is necessary, however, to arbitrarily cut off the distribution at some finite energy to obtain meaningful results. The $\kappa = \Sigma_s$ limit normally implies

a cutoff in the ev to Kev range at energies where $\Sigma_a(1/v) << \Sigma_s$ = constant; even this range may be too high. (The cadmium shutter technique implies the source energy is cut off at 0.62 ev. The resultant limit is shown in Figure 6.) Perhaps a more meaningful (but still somewhat arbitrary) limit is one which includes all but a numerically negligible number of source neutrons. If we require that only one activation out of one thousand in a 1/v detector near the source is caused by higher energy neutrons, a cutoff energy of 8.7 kT_o is obtained. At this energy, Σ_s for D_2O is slightly higher than the free atom value and the magnitude of the absorption cross section of the poisoned D_2O is comparable. This limit is shown in Figure 6 and is seen to be consistent with the experimental values.

REFERENCES

1. N. P. Baumann. "Determination of Diffusion Coefficients for Thermal Neutrons in D_2O at 20, 100, 165, and 220°C." *Nucl. Sci. and Eng. 14,* 179 (1962).

2. H. C. Honeck and P. Michael. "A Remark on the Measurement of the Diffusion Coefficient for Thermal Neutrons." *Nucl. Sci. and Eng. 16,* 140 (1963).

3. H. C. Honeck. *On the Calculation of Thermal Neutron Diffusion Parameters.* BNL-719 (C-32), Vol. IV, p. 1186, Brookhaven National Laboratory, Upton, N. Y. (1962).

4. J. W. Daughtry and A. W. Waltner. "Temperature Dependence of the Thermal Neutron Properties of D_2O." *Trans. Am. Nucl. Soc. 7(2),* 232 (1964).

5. G. Kussmaul and H. Meister. "Thermal Neutron Diffusion Parameters of Heavy Water." *Reactor Sci. and Technol. 17,* 411 (1963).

6. B. K. Malaviya, I. Kaplan, D. O. Lanning, A. E. Profio, and T. J. Thompson. *Studies of Reactivity and Related Parameters in Slightly Enriched Uranium, Heavy Water Lattices.* USAEC Report MITNE-49, Massachusetts Institute of Technology, Cambridge, Mass. (1964).

7. N. Corngold. "Some Transient Phenomena in Thermalization-Theory." *Nucl. Sci. and Eng. 19,* 80 (1964).

8. W. V. Baxter. *A Monte Carlo Code for the Transport of Neutrons.* USAEC Report DP-446, E. I. du Pont de Nemours and Co., Savannah River Laboratory, Aiken, S. C. (1959).

9. H. C. Honeck. *THERMOS. A Thermalization Transport Theory Code for Reactor Lattice Calculations.* USAEC Report BNL-5826, Brookhaven National Laboratory, Upton, N. Y. (1961).

10. E. Starr and J. Koppel. "Determination of Diffusion Hardening in Water." *Nucl. Sci. and Eng. 14,* 224 (1962).

11. E. Gon, L. Lidofsky, and H. Goldstein. "Pulsed-Source Measurements of Neutron-Diffusion Parameters in Water." *Trans. Am. Nucl. Soc. 8(1),* 274 (1965).

12. J. R. Stehn, M. D. Goldberg, B. A. Magurno, and R. Wiener-Chasman. *Neutron Cross Sections.* 2nd ed., Supplement No. 2, USAEC Report BNL-325, Brookhaven National Laboratory, Upton, N. Y. (1964).

13. S. Glasstone and M. C. Edlund. *The Elements of Nuclear Reactor Theory.* p. 281, D. Van Nostrand Co. (1952).

14. N. G. Sjostrand. "On the Theory Underlying Diffusion Measurements with Pulsed Neutron Sources. *Arkiv for Fysik Band 15, nr 12,* 147 (1959).

15. A. Radkowsky. *Temperature Dependence of Thermal Transport Mean Free Path from Experimental Data on Scattering Cross Section of Water.* USAEC Report ANL-4476, Argonne National Laboratory, Lemont, Ill. (1950).

16. R. C. Axtmann, L. A. Heinrich, R. C. Robinson, O. A. Towler, and J. W. Wade. *Initial Operation of the Standard Pile.* USAEC Report DP-32, E. I. du Pont de Nemours and Co., Savannah River Laboratory, Aiken, S. C. (1953).

17. L. C. Schmid and W. P. Stinson. *Lutetium as a Spectral Index Detector.* USAEC Report HW-66319, General Electric Co., Hanford Atomic Products Operation, Richland, Washington (1960).

18. W. M. Lopez and J. R. Beyster. "Measurement of Neutron Diffusion Parameters in Water by the Pulsed Neutron Method." *Nucl. Sci. and Eng. 12,* 190 (1962).

19. R. Peierls. "Statistical Error in Counting Experiments." *Proc. Roy. Soc. (London) A149,* 467 (1955).

20. J. I. Paulk and M. B. Stroud. *"PEX Code."* Private communication.

21. P. F. Nichols, E. G. Bilpuch, and H. W. Newson. "s- and p-Wave Neutron Spectroscopy, Part IV. Experimental Methods in the kev Region." *Annals of Physics 8,* 250 (1959).

22. N. P. Baumann and M. B. Stroud. "Self-Shielding of Detector Foils in Reactor Fluxes." *Nucleonics 23(8),* 98 (1965).

23. R. C. Kryter, G. P. Calame, R. R. Fullwood, and E. R. Gaerttner. "Measurement and Analysis of Time-Dependent Neutron Spectra in D_2O." *Trans. Am. Nucl. Soc. 8(1),* 276 (1965).

24. M. M. Bretscher and J. F. Meyer. "Diffusion Heating and Cooling of Thermal Neutrons in Water." *Proc. Indiana Acad. Sci. 73,* 210 (1964).

25. H. P. Flatt and D. C. Baller. *AIM-5, A Multigroup, One-Dimensional Diffusion Equation Code.* USAEC Report NAA-SR-4694, Atomics Int. Div., N. Am. Avia., Inc., Canoga Park, Calif. (1960).

26. A. K. Ghatak and H. C. Honeck. "Transient Spectra in Graphite." *J. Nucl. Energy 19,* 1 (1965).

27. E. Starr and G. A. Price. *Measurement of the Diffusion Parameters of Graphite and Graphite-Bismuth by Pulsed Neutron Methods.* USAEC Report BNL-719, (C32), Vol. III, p. 1034, Brookhaven National Laboratory, Upton, N. Y. (1962).

28. J. I. Paulk and A. W. Waltner. "The Diffusion Parameters of Heavy- and Light-Water Mixtures at Different Temperatures by Pulsed-Neutron Methods." *Trans. Am. Nucl. Soc. 5(2),* 387 (1962).

29. H. D. Brown. *Neutron Energy Spectra in Water.* USAEC Report DP-64, E. I. du Pont de Nemours and Co., Savannah River Laboratory, Aiken, S. C. (1956).

30. K. Burkart. *On the Hardening of Thermal Neutron Spectra in Water and Boric Acid Solution.* USAEC Report KFK 294, Gesellschaft fur Kernforschung, Karlsruhe (1965).

31. G. S. Stanford and K. E. Plumlee. "Linear Relationship Between Cadmium Ratio and Reactor Core Composition." *Trans. Am. Nucl. Soc. 8(1),* 270 (1965).

32. C. H. Westcott. *Effective Cross Section Values for Well-Moderated Thermal Reactor Spectra.* USAEC Report CRRP-960 (AECL-1101), Atomic Energy of Canada Ltd., Chalk River, Ont. (1960).

33. H. D. Brown and D. S. St. John. *Neutron Energy Spectrum in D_2O.* USAEC Report DP-33, E. I. du Pont de Nemours and Co., Savannah River Laboratory, Aiken, S. C. (1954).

34. N. Corngold and P. Michael. "Some Transient Phenomena in Thermalization-Implications for Experiment." *Nucl. Sci. and Eng. 19,* 91 (1964).

35. N. Corngold and K. Durgun. "The Decay Constant of a Neutron Pulse." *Nucl. Sci. and Eng. 25,* 450 (1966).

APPENDIX

CORRECTIONS TO PULSED MEASUREMENTS IN D_2O

1. Fix

$$\delta_z(D_2O) = 0.7104\ \lambda_{tr} = 1.79 \text{ cm at } 29^\circ\text{C}.^1$$

2. Compute aluminum reflector savings for side, top, and bottom:

$$\delta(Al) = d(Al)\Sigma(Al)^{tr}/\Sigma(D_2O)^{tr} = 0.212\ d(Al)$$

3. Compute extrapolation distance for curved surface of radius R:

$$\delta_r(D_2O) = \delta_z(D_2O)\left[\frac{1}{1.0 + 0.5[\delta_z(D_2O)/R]}\right]$$

4. Compute B^2 including aluminum:

$$B^2 = B_r^2 + B_z^2 = \left[\frac{2.405}{R + \delta_r(D_2O) + \delta_s(Al)}\right]^2 + \left[\frac{3.1416}{H + 2\,\delta_z(D_2O) + \delta_t(Al) + \delta_b(Al)}\right]^2$$

where H is the moderator height.

5. Divide $(\lambda-\lambda_o)_{T_m}$ by B^2, where T_m is the moderator temperature:

$$\frac{(\lambda-\lambda_o)_{T_m}}{B^2} = (vD)_{eff}^{T_m} \cong v^{T_m} D_{eff}^{T_m}$$

6. Correct for minor deviations of T_m from pulsed reference moderator temperature of 29°C (302°K). The relevant exact equations are:

$$D_{eff}^{29°C} = D_{eff}^{T_m}\left[0.69 + 0.31\left(\frac{T_m}{293}\right)^{\frac{1}{2}}\right]^{-1}\left[0.69 + 0.31\left(\frac{302}{293}\right)^{\frac{1}{2}}\right]$$

$$v^{29°C} = v^{T_m}\left(\frac{302}{T_m}\right)^{\frac{1}{2}}$$

These relations give, for small differences ΔT from 29°C, a fractional change in (vD) of

$$\frac{\Delta(vD)_{eff}^{29°C}}{(vD)_{eff}^{29°C}} \cong 2.16 \times 10^{-3}\ \Delta T$$

7. Compute $\left[\frac{\lambda-\lambda_o}{B^2}\right]_{29°C} = (vD)_{eff}^{T_m} - \Delta(vD) = (vD)_{eff}^{29°C}$

8. Plot $(vD)_{eff}^{29°C}$ and estimate $(vD)_o^{29°C}$ at $B^2 = 0$.

9. $$\frac{(vD)_{eff}^{29°C}}{(vD)_o^{29°C}} = \frac{\left(\frac{T_n}{302}\right)^{\frac{1}{2}}\left[0.69 + 0.31\left(\frac{T_n}{293}\right)^{\frac{1}{2}}\right]}{\left[0.69 + 0.31\left(\frac{302}{293}\right)^{\frac{1}{2}}\right]}$$ where T_n is the neutron temperature.

The ratio on the left is given by the experiment; thus T_n may be solved graphically from the data to evaluate $D_{eff}^{T_n}$ from the equation of Step 6 if T_m is replaced by T_n.

10. Compute new slab type extrapolation distance:

$$\delta_z(D_2O) = 0.7104\ \lambda_{eff}^{tr} = 2.13\ D_{eff}^{T_n}$$

11. Go back to Step 3 and iterate Steps 3 through 10 until convergence is obtained in $(vD)_{eff}^{29°C}$. (Step 2 can be left out of iteration since δ_{Al} is quite small.)